Pergamon

Tetrahedron 58 (2002) 2853–2859

TETRAHEDRON

Furanoid sugar amino acid based peptidomimetics: well-defined solution conformations to gel-like structures

T. K. Chakraborty,* S. Jayaprakash, P. Srinivasu, S. S. Madhavendra, A. Ravi Sankar and A. C. Kunwar*

Organic Division-111, Bioorganic Laboratory, Indian Institute of Chemical Technology, Hyderabad 500 007, India

Received 13 November 2001; revised 9 January 2002; accepted 7 February 2002

Abstract—Furanoid sugar amino acid based peptide and a dimer fold into pseudo β-turn-like structures in DMSO-d_6 with intramolecular H-bonds between LeuNH and sugarOH. In $CDCl_3$, they display a repeating β-turn-type secondary structure at lower concentrations and start to form aggregates that gradually turn into excellent organogels as the concentrations are increased, a phenomenon observed for the first time in sugar amino acid containing peptides.

1. Introduction

In recent years chemists have synthesized a large variety of oligomeric compounds with an aim to mimic the structures and functions of biopolymers.[1] Rationally designed monomeric units are threaded together in specific sequences by iterative synthetic methods leading to many novel homo- and heteropolymers with architecturally beautiful three dimensional structures and useful properties. This has led to an ever-expanding repertoire of structurally diverse synthetic building blocks that were developed to instill desirable geometrical biases in the designer molecules. Sugar amino acids represent an important class of such conformationally constrained templates that have been used extensively in recent years in many peptidomimetic studies[2] and have emerged as an important class of synthetic monomers leading to many de novo oligomeric libraries.[3] As part of our ongoing project on sugar amino acid based molecular designs, we report here detailed structural studies of two glucose-derived furanoid sugar amino acid [6-amino-2,5-anhydro-6-deoxy-D-gluconic acid (**1**, Gaa)] based peptidomimetics, Boc-Gaa-Phe-Leu-OMe **3** and its dimer **4**. Conformational analysis of compounds **3** and **4** by various NMR spectroscopic techniques revealed that, in a polar solvent like DMSO-d_6, they folded into pseudo β-turn-like structures with intramolecular H-bonds between LeuNH and sugarOH, as depicted schematically in structure **A**. In a nonpolar solvent like $CDCl_3$, they displayed a repeating β-turn-type secondary structure at lower concentrations and started forming aggregates that gradually turned into excellent organogels as the concentrations were increased. To the best of our knowledge, this is the first report on the formation of sugar amino acid based organogels.

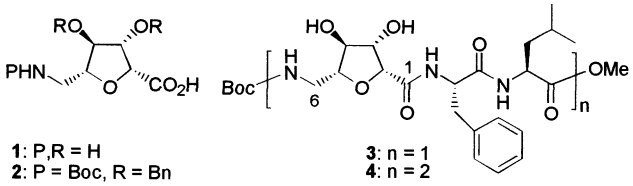

1: P,R = H
2: P = Boc, R = Bn

3: n = 1
4: n = 2

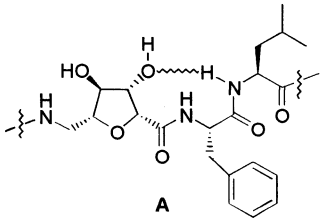

A

2. Results and discussion

2.1. Synthesis of peptidomimetics 3 and 4

Compounds **3** and **4** were synthesized by coupling first *N*-Boc-*O*-benzyl derivative of Gaa (**2**) with H_2N-Phe-Leu-OMe under standard solution phase peptide synthesis conditions using 1-ethyl-3-(3-(dimethylamino)propyl)-carbodiimide hydrochloride (EDCI) and 1-hydroxybenzotriazole (HOBt) as coupling agents and amine-free dry DMF and dry CH_2Cl_2 as solvents.[4] One portion of the resulting peptide Boc-Gaa(Bn_2)-Phe-Leu-OMe was saponified to free the acid terminal that was reacted next with H_2N-Gaa(Bn_2)-Phe-Leu-OMe, prepared by Boc-deprotection of the other part, to furnish the protected dimer. Final debenzylations were carried out by hydrogenation using

Keywords: peptide mimetics; hydrogen bonding; conformation; NMR; organogels.

* Corresponding authors. Tel.: +91-40-719-3154; fax: +91-40-716-0757; e-mail: chakraborty@iict.ap.nic.in

0040–4020/02/$ - see front matter
PII: S0040-4020(02)00158-8

Table 1. ^{1}H Chemical shifts (δ) in ppm, coupling constants (J) in Hz and temperature coefficients of the amide protons ($\Delta\delta/\Delta T$) in ppb/K of **3** in DMSO-d_6 (500 MHz)

Protons	Phe	Leu
NH	8.32 (d, $^3J_{NH-\alpha H}$=9.8 Hz)	7.78 (d, $^3J_{NH-\alpha H}$=8.05 Hz)
CαH	4.65 (ddd)	4.30 (ddd)
CβH (*pro-S*)	3.38 (dd, $^3J_{\alpha-\beta(pro-S)}$=3.60 Hz)	1.44 (ddd, $^3J_{\alpha-\beta(pro-S)}$=4.7 Hz)
CβH (*pro-R*)	2.85 (dd, $J_{\alpha-\beta(pro-R)}$=10.8 Hz, $^2J_{\beta(pro-R)-\beta(pro-S)}$=14.3 Hz)	1.51 (ddd, $^3J_{\alpha-\beta(pro-R)}$=10.5 Hz, $^2J_{\beta(pro-R)-\beta(pro-S)}$=12.7 Hz)
CγH		1.71 (ddt, $J_{\gamma-\beta(pro-S)}$=9.7 Hz, $J_{\gamma-\beta(pro-R)}$=4.9 Hz)
CδH		0.82 (d, CH_3(*pro-R*)), 0.80 (d, CH_3(*pro-S*)), ($J_{\gamma-\delta(pro-R)}$, $J_{\gamma-\delta(pro-R)}$=6.5 Hz)
Others	7.15–7.22 (m, Ar-H)	
$-\Delta\delta/\Delta T$ (ppb/K) for NH	8.1	1.7

Gaa: NH=7.08 (bt), 5.89 (d, C3–OH, J_{H3-OH}=3.3 Hz), 5.29 (d, C4–OH, J_{H4-OH}=3.4 Hz), 4.27 (d, C2–H, J_{H2-H3}=3.7 Hz), 4.04 (C3–H, J_{H3-H4}=3.8 Hz), 3.79 (C5–H, J_{H4-H5}=3.1 Hz, $J_{H5-H6(pro-R)}$=9.7 Hz, $J_{H5-H6(pro-S)}$=3.0 Hz), 3.76 (C4–H), 3.46 (C6–H(*pro-R*), J_{H6-NH}=7.0 Hz), 2.96 (C6–H(*pro-S*), $J_{H6'-NH}$=5.9 Hz); $-\Delta\delta/\Delta T$ (ppb/K) for GaaNH=8.1

$Pd(OH)_2$–C as catalyst in MeOH–EtOAc to furnish **3** and **4** in excellent overall yields.

2.2. Conformational analysis. NMR spectroscopic studies

NMR spectroscopic studies of **3** and **4** were carried out both in polar (DMSO-d_6) and apolar solvents ($CDCl_3$). The ^{1}H chemical shifts, coupling constants and temperature coefficients ($\Delta\delta/\Delta T$) of the amide protons of **3** and **4** in DMSO-d_6 are listed in Tables 1 and 2, respectively. Our earlier studies[2d,4] on larger peptides containing **3** in DMSO-d_6 showed a very unusual β-turn like structure as shown in structure **A**, with a fairly rigid Leu side chain. It is interesting to note that a smaller peptide **3** also shows a very similar turn like structure in DMSO-d_6, as shown schematically in Fig. 1, with an intramolecular H-bond between LeuNH and sugarC3–OH. The structure was supported by rOe cross-peaks between LeuNH-GaaC3–OH, LeuδCH$_3$(*pro-R*)-GaaC3–OH, LeuβH(*pro-R*)-GaaC3–OH, LeuγH-GaaC6-H(*pro-R*), PheNH-LeuNH, LeuαH-LeuδCH$_3$(*pro-S*) and PheαH-LeuNH. The temperature coefficient for Leu amide proton chemical shift ($\Delta\delta/\Delta T$) of -1.7 ppb/K, further confirmed its participation in intramolecular hydrogen bond. The Leu side-chain was fairly rigid as reflected by $^3J_{\alpha-\beta(pro-R)}$=10.5 Hz, $^3J_{\alpha-\beta(pro-S)}$=4.7 Hz, $^3J_{\beta(pro-R)-\gamma}$=4.9 Hz and $^3J_{\beta(pro-S)-\gamma}$=9.7 Hz as well as a significant nOe between LeuαH-LeuδCH$_3$(*pro-S*). Leu side-chain has about 77% population of g^- isomer about χ_1 and about 59% rotamer population with *anti* relationship between βH(*pro-S*) and γH about χ_2. For Phe also there was very large population of g^- isomer about χ_1 (80%). There was no indication of other amide protons participating in hydrogen bonding having very large magnitudes of $\Delta\delta/\Delta T$, -8.1 ppb/K for both GaaNH and PheNH. The small values of couplings between the protons in the sugar ring and the nOe between GaaC2–H and GaaC5–H are consistent with an envelope conformation of the furanoid ring with GaaC3 being the flap of the envelope.

The peptide **4**, in DMSO-d_6, showed very similar behavior for individual Gaa-Phe-Leu units as it was seen in **3**. However, due to overlap of resonances, several of the details could not be obtained unambiguously and accurately. Yet the signatures of the turns in the individual Gaa-Phe-Leu segments were unmistakably seen. The $\Delta\delta/\Delta T$ for Leu(I)NH and Leu(II)NH were -2.7 and -2.2 ppb/K, respectively, again indicating the presence of hydrogen bonds of moderate strengths. The assignments of the resonances to two fragments of Gaa-Phe-Leu were obtained by the ROESY peaks between Leu(I)αH-Gaa(II)NH and Leu(I)NH-Gaa(II)NH. The proximities of both the LeuNH to the corresponding sugar C3–OH in the ROESY spectrum further confirmed that LeuNH⟶GaaC3–OH hydrogen bonds are formed for both the Gaa-Phe-Leu units. Additional cross peaks in the ROESY spectrum, like Leu(II)γH-Gaa(II)C6-H(*pro-R*), Leu(II)δCH$_3$(*pro-R*)-Gaa(II)C6-H(*pro-R*), Leu(II)βH-Gaa(II)C3–OH,

Table 2. ^{1}H Chemical shifts (δ) in ppm, coupling constants (J) in Hz and temperature coefficients of the amide protons ($\Delta\delta/\Delta T$) in ppb/K of **4** in DMSO-d_6 (500 MHz)

Protons	Phe(I)	Leu(I)	Phe(II)	Leu(II)
NH	8.12 (d, $^3J_{NH-\alpha H}$=8.8 Hz)	7.64 (d, $^3J_{NH-\alpha H}$=7.7 Hz)	8.11 (d, $J_{NH-\alpha H}$=9.2 Hz)	7.86 (d, $J_{NH-\alpha H}$=8.32 Hz)
CαH	4.63 (dt, $^3J_{\alpha-\beta(pro-S)}$=4.0 Hz, $^3J_{\alpha-\beta(pro-R)}$=9.4 Hz)	4.36 (dt, $^3J_{\alpha-\beta(pro-S)}$=4.9 Hz, $^3J_{\alpha-\beta(pro-R)}$=9.1 Hz)	4.59 (dt, $^3J_{\alpha-\beta(pro-S)}$=3.7 Hz, $^3J_{\alpha-\beta(pro-R)}$=9.8 Hz)	4.27 (dt, $^3J_{\alpha-\beta(pro-S)}$=5.1 Hz, $^3J_{\alpha-\beta(pro-R)}$=8.2 Hz)
CβH (*pro-S*)	3.27 (m)	1.45 (m, $J_{\gamma-\beta(pro-S)}$=9.1 Hz)	3.28 (dd)	1.50 (m)
CβH (*pro-R*)	2.94 ($^2J_{\beta(pro-R)-\beta(pro-S)}$=13.9 Hz)	1.50 (m, $J_{\gamma\beta}$=5.4 Hz)	2.93 ($^2J_{\beta(pro-R)-\beta(pro-S)}$=14.2 Hz)	1.50 (m)
CγH		1.66 (m, $J_{\gamma\delta}$=6.4 Hz)		1.66 (m, $J_{\gamma\delta}$=6.4 Hz)
CδH		0.82 (d, CH_3(*pro-R*)), 0.79 (d, CH_3(*pro-S*))		0.82 (d, CH_3(*pro-R*)), 0.78 (d, CH_3(*pro-S*))
Others	7.14–7.28 (m, Ar-H)	3.68 (s, CO_2CH_3)	7.14–7.28 (m, Ar-H)	3.69 (s, CO_2CH_3)
$-\Delta\delta/\Delta T$ (ppb/K) for NH	5.5	2.7	5.5	2.2

Gaa(I): NH=6.93 (t, ^3J=6.4 Hz), C6–H(*pro-R*)=3.41, C6–H(*pro-S*)=3.00, C5–H=3.83, C4–H=3.81, C3–H=4.06, C2–H=4.30, C3–OH=5.49, C4–OH=5.18; $-\Delta\delta/\Delta T$ (ppb/K) for NH=7.5
Gaa(II): NH=7.77 (t, ^3J=6.8 Hz), C6–H(*pro-R*)=3.72, C6–H(*pro-S*)=3.02, C5–H=3.83, C4–H=3.81, C3–H=4.08, C2–H=4.26, C3–OH=5.59, C4–OH=5.18; $-\Delta\delta/\Delta T$ (ppb/K) for NH=5.7

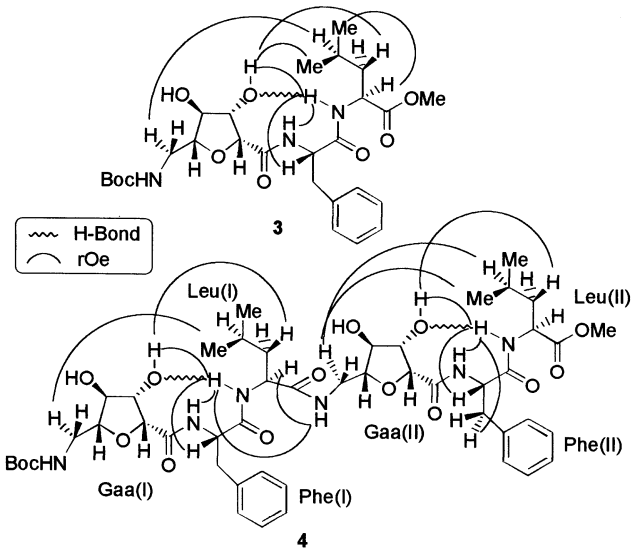

Figure 1. Schematic representation of the hydrogen bonded structures of **3** and **4** in DMSO-d_6 with the long range rOes seen in its ROESY spectrum.

Leu(I)NH-Gaa(I)C3–OH, Leu(I)βH(*pro-R*)-Gaa(I)C3–OH, Phe(I)NH-Leu(I)NH, Phe(II)NH-Leu(II)NH, Leu(II)NH-Phe(II)αH, Gaa(II)NH-Leu(I)αH, Leu(I)NH-Phe(I)αH, Leu(II)NH-Phe(II)βH(*pro-S*), Leu(I)δCH$_3$(*pro-R*)-Gaa(I)C6-H(*pro-R*) were observed supporting the presence of unusual turn like structures in both the fragments, as illustrated in Fig. 1. Due to spectral overlap relevant couplings of only one Leu side-chain were obtained, with any degree of accuracy. It showed that the Leu(I) side-chain was rigid. We prefer not to over interpret these couplings.

The cross-peak intensities in the ROESY spectra of **3** and **4** in DMSO-d_6, shown schematically in Fig. 1, were used for obtaining the restraints in the MD calculations. Based on the cross-peak intensities, the nOes between various protons were classified as strong, medium, weak and very weak. These were translated into distance restraints as 2.0–2.8 Å for strong, 2.0–3.5 Å for medium, 2.0–4.0 Å for weak and 2.0–4.5 Å for very weak nOes.[5] Several long-range distance constraints, torsional restraints and an H-bonding restraint were used in the energy calculations. The result derived from the 120 ps MD run for compound **3** is shown in Fig. 2. The superimposed display of the 20 structures sampled at regular intervals of 6 ps during a 120 ps MD run, subsequently annealed, energy-minimized and superimposed aligning the hydrogen bonded parts clearly reveal cyclic conformations of **3** involving hydrogen bonds between LeuNH and sugarC3–OH. In the dimmer **4**, the same pattern is observed in both Gaa-Phe-Leu units.

Fleet et al. have shown that oligomers of some of the sugar amino acids take a β-bend ribbon spiral structure in $CDCl_3$ consisting of successive β-turns.[3b–d] In view of this, we also undertook NMR studies of peptide **3** and **4** in $CDCl_3$, the data for which are listed in Tables 3 and 4, respectively. In peptide **4**, all the amide resonances in $CDCl_3$, with the exception of Gaa(I)NH, appeared at very low field (>7 ppm) implying their participation in hydrogen bonding. Solvent titration studies (Table 5) showed that addition of DMSO-d_6, a hydrogen bonding solvent, did not change these amide chemical shifts by large amounts confirming further their participation in hydrogen bonding.[6] In the second Gaa-Phe-Leu fragment in peptide **4**, we also observed the proximity of Leu(II)NH to Gaa(II)C3–OH, which indicated a NH⟶C3–OH hydrogen bond. The large temperature coefficients of −12 and −10 ppb/K for Gaa(II)NH and Phe(II)NH, respectively, further supported the preponderance of structures with these amides participating in hydrogen bonding.[6b] These hydrogen bonds imply the presence of β-turns as observed by Fleet[3b–d] and illustrated schematically in the Fig. 3. Due to the broadening of spectral lines, we were unable to obtain other details of hydrogen bonding of amides from the ROESY spectra.

In peptide **3** also the participation of PheNH and LeuNH in hydrogen bonding in $CDCl_3$, as shown in Fig. 3, were supported by both their low field chemical shifts and moderate variation of these shifts in solvent titration as shown in Table 5.

All the above NMR spectroscopic studies in $CDCl_3$ were carried out with very low concentrations of the peptides, ~0.6 mM for **3** and ~0.3 mM for **4**. With increasing concentrations of the peptides, all the amide resonances showed monotonic downfield shifts indicating their aggregation in $CDCl_3$. As the concentrations were gradually increased, at nearly 5–6 mM both compounds started forming gels.

Solutions of **3** and **4** in $CHCl_3$ (<1 wt% gelators) turned into gels upon standing at ambient temperature. To examine the

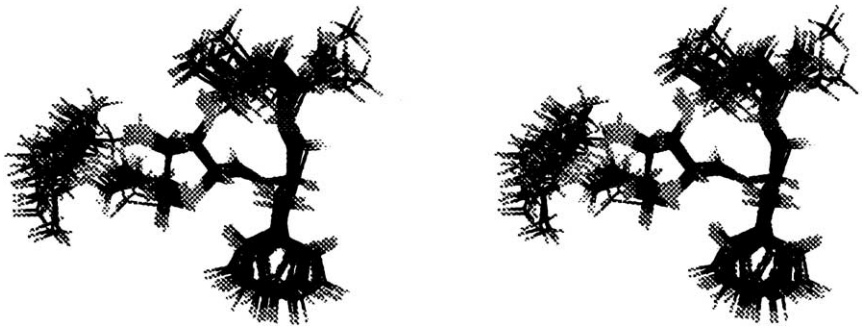

Figure 2. Stereoview of the 20 superimposed structures of **3** in DMSO-d_6, sampled at 6 ps intervals during 120 ps MD simulations, subsequently annealed, energy-minimized and superimposed aligning the hydrogen bonded parts, displaying folded conformations with intramolecular hydrogen bonds between LeuNH and sugarC3–OH.

Table 3. ^{1}H Chemical shifts (δ) in ppm and coupling constants (J) in Hz of **3** in $CDCl_3$ (500 MHz)

Protons	Phe	Leu
NH	7.83 (d, $^3J_{NH-\alpha H}$=8.4 Hz)	7.08 (d, $^3J_{NH-\alpha H}$=8.5 Hz)
CαH	4.77 (dt, $^3J_{\alpha-\beta(pro\text{-}S)}$=6.60 Hz, $^3J_{\alpha-\beta(pro\text{-}R)}$=8.4 Hz)	4.65 (ddd, $^3J_{\alpha-\beta(pro\text{-}S)}$=4.9 Hz, $^3J_{\alpha-\beta(pro\text{-}R)}$=9.4 Hz)
CβH (down)	3.25 (m)	1.47 (m)
CγH	1.61 (m)	
CδH		0.90 (d, $J_{\gamma-\delta(pro\text{-}R)}$=6.5 Hz), 0.86 (d, $J_{\gamma-\delta(pro\text{-}S)}$=6.5 Hz)
Others	7.23–7.33 (m, Ar-H)	3.69 (CO_2CH_3)

Gaa: NH=4.81 (bt), 4.24 (d, C3–OH, J_{H3-OH}=3.3 Hz), 2.15 (d, C4–OH), 4.62 (d, C2–H, J_{H2-H3}=4.0 Hz), 4.45 (C3–H, J_{H3-H4}=3.7 Hz), 4.01 (C5–H, J_{H4-H5}=2.7 Hz, $J_{H5-H6(pro\text{-}R)}$=9.1 Hz, $J_{H5-H6(pro\text{-}S)}$=4.4 Hz), 4.05 (C4–H), 3.52 (C6–H(*pro-R*), J_{H6-NH}=6.7 Hz), 3.19 (C6–H(*pro-S*), $J_{H6'-NH}$=6.7 Hz)

Due to broadening of lines some of the couplings could not be obtained.

Table 4. ^{1}H Chemical shifts (δ) in ppm, coupling constants (J) in Hz and temperature coefficients of the amide protons ($\Delta\delta/\Delta T$) in ppb/K of **4** in $CDCl_3$ (500 MHz)

Protons	Phe(I)	Leu(I)	Phe(II)	Leu(II)
NH	7.69 ($J_{NH-\alpha H}$=7.8 Hz)	7.37 ($J_{NH-\alpha H}$=8.2 Hz)	8.14 ($J_{NH-\alpha H}$=8.4 Hz)	7.54
CαH	4.74	4.45	4.62	4.42
CβH	3.18	1.48	3.24	1.4
CγH				1.6
CδH		0.83 (d)		0.83(d)
Others	7.14–7.28 (m, ArH)	3.68 (s, CO_2CH_3)	7.14–7.28 (m, Ar-H)	3.69 (s, CO_2CH_3)
$-\Delta\delta/\Delta$T (ppb/K) for NH	2.0	8.0	10.0	4.5

Gaa(I): NH=5.02 (bt), C6–H(*pro-R*)=3.52, C6–H(*pro-S*)=3.10, C5–H=3.96, C4–H=3.93, C3–H=4.31, C2–H=4.51, C3–OH=4.84, C4–OH=4.84
Gaa(II): NH=7.28 (bt), C6–H(*pro-R*)=3.48, C6–H(*pro-S*)=3.20, C5–H=3.93, C4–H=3.95, C3–H=4.30, C2–H=4.50, C3–OH=5.47, C4–OH=4.55.12; $-\Delta\delta/\Delta T$ (ppb/K) for NH=12.0

Due to broadening of lines some of the couplings could not be obtained.

Table 5. Changes in the chemical shifts of the amide protons ($\Delta\delta$ in ppm) on addition of DMSO-d_6 (200 μL) to solutions of **3** and **4** in $CDCl_3$ (0.6 mL)

Compound	NH	$\Delta\delta$ (ppm)
3	Gaa	1.56
	Phe	0.49
	Leu	0.61
4	Gaa(I)	1.48
	Phe(I)	0.05
	Leu(I)	0.58
	Gaa(II)	0.32
	Phe(II)	0.14
	Leu(II)	0.69

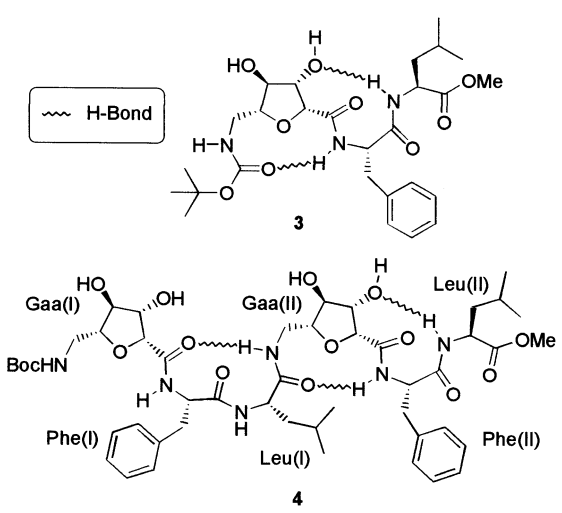

Figure 3. Schematic representation of the possible hydrogen bonded structures of **3** and **4** in $CDCl_3$.

morphology of the gels, scanning electron microscopic (SEM) analysis of the xerogels was carried out. Wet gels were placed on aluminium stubs, air dried, gold coated in HUS-5GB vacuum evaporator and observed in Hitachi S-520 Scanning Electron Microscope at an acceleration voltage of 10 kV.

There was no significant size reduction in the gel obtained from **3** after drying. The gel was porous and the 3D structure was well preserved, which was evident by the clear-cut open cell structure with each cell having at least two pores beneath (Fig. 4a). The pore size ranged from ca. 1 to 4.5 μm. Smaller pores (<0.3 μm) were regular (spherical) in shape. The cell walls comprised of fibres of ca. 0.3 μm diameter, which formed a dense network. At few places, these fibres formed macrofibres of ca. 2 μm diameter (Fig. 4b).

In case of **4**, a drastic size reduction in the gel was observed on drying. The SEM image of the gel from **4** (Fig. 4c) revealed a compact three-dimensional fibrous structure with an average fibre diameter of ca. 1.5 μm. While the fibres were straight where they were dense, they were wavy and tending to form helices where they were loose (Fig. 4d).

The aggregation phenomena observed here that led to the formation of excellent organogels could possibly be attributed to the amphipathic nature of these sugar amino acid based peptides that contain the polar hydroxyl groups on sugar rings along with the Phe and Leu hydrophobic side-chains. The intermolecular hydrogen bondings in nonpolar organic solvent in addition with other supramolecular

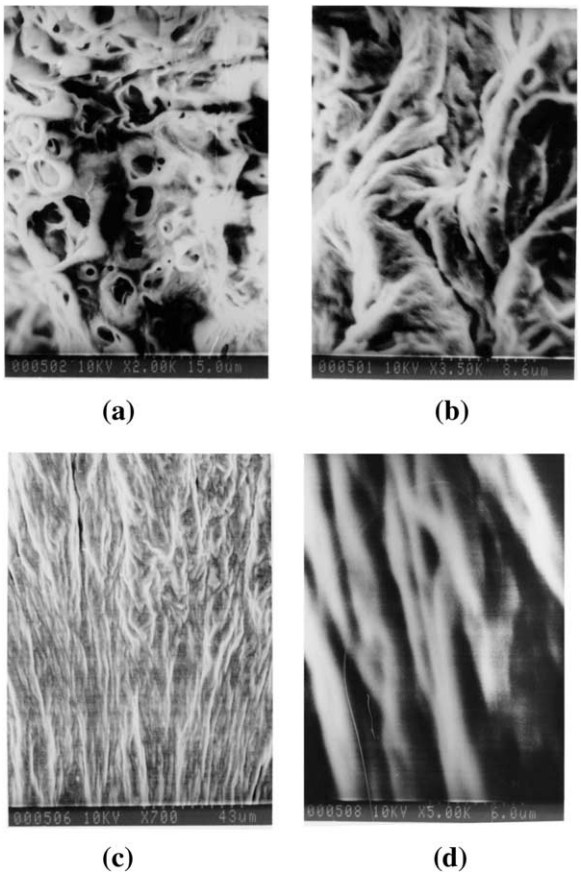

Figure 4. SEM pictures of xerogels from **3** (a and b) and **4** (c and d) in $CHCl_3$.

noncovalent forces, like possible aromatic stackings and electrostatic interactions, might have resulted in the formation of aggregates that entrapped solvent molecules to create gelatinous structure. Sugar-based gelators have an advantage over others as one can choose from a large repertoire of carbohydrate library to design an appropriate gelator that is most suitable for a particular solvent.

In conclusion, this paper demonstrates further the abilities of sugar amino acids to introduce interesting secondary structures in peptides that can have many potential applications in designing novel peptidomimetics. Also noteworthy is their tendency to form organogels in nonpolar solvents, observed for the first time in any sugar amino acid based molecular designs. Development of new low molecular weight gelators, especially, of organic solvents is of intense current interest as the diverse nanostructures displayed by these organogels have many potential practical utilities in the development of new functional materials.[7] The gels formed by sugar amino acid based peptidomimetics are also expected to find many useful applications.

3. Experimental

3.1. General procedures

All reactions were carried out in oven or flame-dried glassware with magnetic stirring under nitrogen atmosphere using dry, freshly distilled solvents, unless otherwise noted. Reactions were monitored by thin layer chromatography (TLC) carried out on 0.25 mm silica gel plates with UV light, I_2, 7% ethanolic phosphomolybdic acid-heat and 2.5% ethanolic anisaldehyde (with 1% AcOH and 3.3% conc. H_2SO_4)-heat as developing agents. Silica gel finer than 200 mesh was used for flash column chromatography. Yields refer to chromatographically and spectroscopically homogeneous materials unless otherwise stated. Melting points are uncorrected. IR spectra were recorded as neat liquids or KBr pellets. Mass spectra were obtained under liquid secondary ion mass spectrometric (LSIMS) technique.

3.2. NMR Spectroscopy

NMR spectra were recorded on 500 MHz spectrometers at 30°C with 7–10 mM solutions in appropriate solvents using tetramethylsilane as internal standard or the solvent signals as secondary standards and the chemical shifts are shown in δ scales. Multiplicities of NMR signals are designated as s (singlet), d (doublet), t (triplet), q (quartet), br (broad), m (multiplet, for unresolved lines), etc. ^{13}C NMR spectra were recorded with complete proton decoupling. The assignments were carried out with the help of two-dimensional total correlation spectroscopy (TOCSY).[8] For some cases the rotating frame nuclear Overhauser effect spectroscopy (ROESY) experiments,[8] which provide the information on the proximity of protons, were additionally used to confirm the assignments made. All the experiments were carried out in the phase sensitive mode using the procedure of States et al.[9] The spectra were acquired with 2×256 or 2×192 free induction decays (FID) containing 8–16 transients with relaxation delays of 1.5–2.0 s. The ROESY experiments were performed with mixing time of 0.3 s. For ROESY experiments a spin-locking field of about 2 kHz was used. The TOCSY experiments were performed with the spin locking fields of about 10 kHz and a mixing time of 0.08 s. The two-dimensional data were processed with gaussian apodization in both the dimensions. The chemical shifts, coupling constants and temperature coefficients ($\Delta\delta/\Delta T$) of amide proton chemical shifts of **3** and **4** in DMSO-d_6 and $CDCl_3$ are given in Tables 1–4. To obtain the temperature coefficients of NH-chemical shifts in DMSO-d_6, the spectra were recorded between 30 and 70°C.

3.3. Molecular dynamics

All molecular mechanics/dynamics calculations were carried out using Sybyl 6.7 program on a Silicon Graphics O2 workstation. The Tripos force field with default parameters was used throughout the simulations. A dielectric constant of 47 Debye was used in all minimizations as well as MD runs. Minimizations were done first with steepest decent, followed by conjugate gradient methods for a maximum of 2000 iterations each or RMS deviation of 0.005 kcal/mol, whichever was earlier. The energy-minimized structures were then subjected to MD simulations. A number of inter-atomic distances and torsional angle constraints[10] obtained from NMR data in DMSO-d_6 including the ω dihedrals, all of which were fixed as *trans*, were used as restraints in the minimization as well as MD runs. Distance constraints with a force constant of 15 kcal/Å

were applied in the form of a flat-bottom potential well with a common lower bound of 2.0 Å and an upper bound of 2.8, 3.5, 4.0 and 4.5 Å, in accordance with the nOe intensities. Force constants of 30 kcal/Å and 5 kcal/rad were employed for H-bond distance and dihedral angle constraints, respectively. The energy-minimized structure was subjected to constrained MD simulations for duration of 120 ps (20 cycles, each of 6 ps period, of the Simulated Annealing protocol). The atomic velocities were applied following Boltzmann distribution about the center of mass to obtain a starting temperature of 1000 K. After simulating for 1 ps at this high temperature, the system temperature was reduced stepwise over a 5 ps period to reach a final temperature of 300 K. Resulting structures were sampled after every 6 ps (one cycle), leading to an ensemble of total 20 structures. The samples were minimized using the above mentioned energy minimization protocol, compared and superimposed as shown in Fig. 2.

3.3.1. Synthesis of 3. A solution of Boc-Gaa(Bn_2)-Phe-Leu-CO_2Me[4] (100 mg, 0.136 mmol) in MeOH–EtOAc (1:1, 2 mL) was hydrogenated in the presence of $Pd(OH)_2$ on C (20%, 50 mg) using a H_2-filled balloon for 5 h. It was then filtered through a short pad of Celite and the filter cake was washed with MeOH. The filtrate and the washings were combined and concentrated in vacuo. Purification by column chromatography (SiO_2, 8% MeOH in $CHCl_3$ eluant) afforded **3** (70 mg, 92%) as a white solid. R_f=0.3 (silica, 8% MeOH in $CHCl_3$); $[\alpha]_D^{20}$=−9.7 (*c* 0.3 in MeOH); mp 186–188°C; IR (KBr): ν_{max} 1725, 1675, 1650 cm^{-1}; ^1H NMR (500 MHz, DMSO-d_6): see Table 1; ^{13}C NMR (125 MHz, DMSO-d_6): δ 172.38, 170.53, 169.03, 156.37, 138.25, 128.68, 128.00, 126.03, 88.12, 82.29, 77.87, 77.73, 77.88, 52.42, 51.74, 50.20, 42.81, 35.96, 28.14, 23.58, 22.65, 20.88; MS (LSIMS): *m/z* (%) 551 (30) [M^+]; HRMS (LSIMS): calcd for $C_{27}H_{42}N_3O_9$ [M^++H]: 552.2921, found: 552.2946.

3.3.2. Synthesis of 4. To a solution of Boc-Gaa(Bn_2)-Phe-Leu-CO_2Me[4] (150 mg, 0.205 mmol) in THF/MeOH/H_2O (3:1:1, 2.5 mL) at 0°C, LiOH/H_2O (25 mg, 0.615 mmol) was added and stirred at the same temperature for 2 h. The reaction mixture was then acidified to pH 2 with 1N HCl. It was diluted with CH_2Cl_2, washed with brine, dried (Na_2SO_4), filtered and concentrated in vacuo to get the acid.

In another round bottom flask a solution of Boc-Gaa(Bn_2)-Phe-Leu-CO_2Me (150 mg, 0.205 mmol) in CH_2Cl_2 (2 mL) was taken. To this trifluoroacetic acid (0.5 mL) was added and stirred at 0°C for 1 h. The reaction mixture was then concentrated in vacuo to give TFA-H_2N-Gaa(Bn_2)-Phe-Leu-CO_2Me.

The above prepared crude acid was dissolved in CH_2Cl_2 (2 mL) and cooled to 0°C. Then it was sequentially treated with HOBt (41 mg, 0.307 mmol) and EDCI (59 mg, 0.307 mmol). After 15 min, TFA-H_2N-Gaa(Bn_2)-Phe-Leu-CO_2Me, prepared above and dissolved in CH_2Cl_2 (2 mL), was added to the reaction mixture followed by DIPEA (0.07 mL, 0.41 mmol). After stirring for 8 h at room temperature, the reaction mixture was diluted with EtOAc, washed with saturated NH_4Cl solution, water, brine, dried (Na_2SO_4), filtered and concentrated in vacuo. Purification by column chromatography (SiO_2, 60% EtOAc in petroleum ether eluant) afforded the Bn-protected dimer (200 mg, 73%), which was used directly in the next step for Bn-deprotection without characterization.

To a solution of the above Bn-protected dimer (200 mg, 0.15 mmol) in MeOH (3 mL), $Pd(OH)_2$ on C (20%, 100 mg) was added and the mixture was hydrogenated under atmospheric pressure using a H_2-filled balloon for 12 h. It was then filtered through a short pad of Celite and the filter cake was washed with MeOH. The filtrate and the washings were combined and concentrated in vacuo. Purification by column chromatography (SiO_2, 10% MeOH in $CHCl_3$ eluant) afforded **4** (123 mg, 85%) as a white solid. R_f=0.5 (silica, 12% MeOH in $CHCl_3$); $[\alpha]_D^{20}$=+7.0 (*c* 0.45 in MeOH); mp 125–128°C; IR (KBr): ν_{max} 1725, 1650, 1600 cm^{-1}; ^1H NMR (500 MHz, DMSO-d_6): see Table 2; ^{13}C NMR (125 MHz, DMSO-d_6): δ 172.43, 170.83, 170.26, 169.56, 169.01, 156.42, 138.36, 138.10, 128.88, 128.75, 128.04, 128.01, 126.04, 87.18, 82.30, 79.08, 77.92, 77.71, 53.16, 51.73, 51.22, 50.42, 42.84, 41.52, 40.72, 36.17, 28.17, 23.78, 22.85, 22.59, 21.34, 21.13; MS (LSIMS): *m/z* (%) 871 (36) [M^++H_2−Boc], 971 (10) [M^++H], 993 (26) [M^++Na].

Acknowledgements

Authors wish to thank Dr M. Vairamani for mass spectroscopic assistance, CSIR, New Delhi for research fellowships (S. J., P. S. and A. R. S.) and DST, New Delhi for financial support (T. K. C.).

References

1. (a) Kirshenbaum, K.; Zuckermann, R. N.; Dill, K. A. *Curr. Opin. Struct. Biol.* **1999**, *9*, 530–535. (b) Barron, A. E.; Zuckermann, R. N. *Curr. Opin. Chem. Biol.* **1999**, *3*, 681–687. (c) Soth, M. J.; Nowick, J. S. *Curr. Opin. Chem. Biol.* **1997**, *1*, 120–129. (d) Gellman, S. H. *Acc. Chem. Res.* **1997**, *31*, 173–180.
2. For some leading references see: (a) Lohof, E.; Planker, E.; Mang, C.; Burkhart, F.; Dechantsreiter, M. A.; Haubner, R.; Wester, H.-J.; Schwaiger, M.; Holzemann, G.; Goodman, S. L.; Kessler, H. *Angew. Chem., Int. Ed. Engl.* **2000**, *39*, 2761–2764 and references therein. (b) van Well, R. M.; Overkleeft, H. S.; Overhand, M.; Carstenen, E. V.; van der Marel, G. A.; van Boom, H. *Tetrahedron Lett.* **2000**, *41*, 9331–9335. (c) Schrey, A.; Vescovi, A.; Knoll, A.; Rickert, C.; Koert, U. *Angew. Chem., Int. Ed. Engl.* **2000**, *39*, 900–902. (d) Chakraborty, T. K.; Jayaprakash, S.; Diwan, P. V.; Nagaraj, R.; Jampani, S. R. B.; Kunwar, A. C. *J. Am. Chem. Soc.* **1998**, *120*, 12962–12963.
3. For some leading references see: (a) Chakraborty, T. K.; Jayapraksh, S.; Srinivasu, P.; Chary, M. G.; Diwan, P. V.; Nagaraj, R.; Ravi Sankar, A.; Kunwar, A. C. *Tetrahedron Lett.* **2000**, *41*, 8167–8171 and references therein. (b) Brittain, D. E. A.; Watterson, M. P.; Claridge, T. D. W.; Smith, M. D.; Fleet, G. W. J. *J. Chem. Soc., Perkin Trans. 1* **2000**, 3655–3665. (c) Hungerford, N. L.; Claridge, T. D. W.; Watterson, M. P.; Aplin, R. T.; Moreno, A.; Fleet, G. W. J. *J. Chem. Soc., Perkin Trans. 1* **2000**, 3666–3679. (d) Hungerford, N. L.;

Fleet, G. W. J. *J. Chem. Soc., Perkin Trans. 1* **2000**, 3680–3685.
4. Chakraborty, T. K.; Ghosh, S.; Jayaprakash, S.; Sarma, J. A. R. P.; Ravikanth, V.; Diwan, P. V.; Nagaraj, R.; Kunwar, A. C. *J. Org. Chem.* **2000**, *65*, 6441–6457.
5. Lian, L. Y.; Barsukov, I. L.; Sutcliffe, M. J.; Sze, K. H.; Roberts, G. C. K. *Methods Enzymol.* **1994**, *239*, 657–700.
6. For leading references on intramolecular hydrogen bonding in small peptides see: (a) Fisk, J. D.; Powell, D. R.; Gellman, S. H. *J. Am. Chem. Soc.* **2000**, *122*, 5443–5447. (b) Chitnumsub, P.; Fiori, W. R.; Lashuel, H. A.; Diaz, H.; Kelly, J. W. *Bioorg. Med. Chem.* **1999**, *7*, 39–59. (c) Gung, B. W.; Zhu, Z. *J. Org. Chem.* **1996**, *61*, 6482–6483. (d) Nowick, J. S.; Abdi, M.; Bellamo, K. A.; Love, J. A.; Martinez, E. J.; Noronha, G.; Smith, E. M.; Ziller, J. W. *J. Am. Chem. Soc.* **1995**, *117*, 89–99.
7. For some recent work and reviews see: (a) Menger, F. M.; Caran, K. L. *J. Am. Chem. Soc.* **2000**, *122*, 11679–11691. (b) Wang, R.; Geiger, C.; Chan, L.; Swanson, B.; Whitten, D. G. *J. Am. Chem. Soc.* **2000**, *122*, 2399–2400. (c) Jung, J. H.; Amaike, M.; Shinkai, S. *Chem. Commun.* **2000**, 2343–2344. (d) van Esch, J. H.; Feringa, B. L. *Angew. Chem., Int. Ed. Engl.* **2000**, *39*, 2263–2266. (e) Maitra, U.; Kumar, P. V.; Chandra, N.; D'Souza, L. J.; Prasanna, M. D.; Raju, A. R. *Chem. Commun.* **1999**, 595–596. (f) Terech, P.; Weiss, R. G. *Chem. Rev.* **1997**, *97*, 3133–3159. (g) Bhattacharya, S.; Acharya, S. N. G.; Raju, A. R. *Chem. Commun.* **1996**, 2101–2102.
8. (a) Cavanagh, J.; Fairbrother, W. J.; Palmer, III, A. G.; Skelton, N. J. *Protein NMR Spectroscopy*; Academic: San Diego, 1996. (b) Wüthrich, K. *NMR of Proteins and Nucleic Acids*; Wiley: New York, 1996.
9. States, D. J.; Haberkorn, R. A.; Ruben, D. J. *J. Magn. Reson.* **1982**, *48*, 286–292.
10. Kessler, H.; Griesinger, C.; Lautz, J.; Müller, A.; van Gunsteren, W. F.; Berendsen, H. J. C. *J. Am. Chem. Soc.* **1988**, *110*, 3393–3396.